RSC Advances

PAPER

View Article Online
View Journal | View Issue

Cite this: *RSC Adv.*, 2023, **13**, 20909

Synthesis and biological evaluation of sulfamoyl benzamide derivatives as selective inhibitors for *h*-NTPDases†

Zahid Hussain Zaigham,‡[a] Saif Ullah,‡[b] Julie Pelletier,[c] Jean Sévigny,[cd] Jamshed Iqbal *[b] and Abbas Hassan *[a]

The aim of this research work is the synthesis of sulfamoyl-benzamides as a selective inhibitor for *h*-NTPDases. Sulfonamides are synthesized in aqueous medium from chlorosulfonylbenzoic acid while carboxamides are synthesized using carbodiimide coupling decorated with different biologically relevant substituents such as *n*-butyl, cyclopropyl, benzylamine, morpholine, and substituted anilines. In addition, sulfonamide-carboxamide derivatives were synthesized having the same substituents on either side. These compounds were screened against *h*-NTPDase activity, a main family of ectonucleotidases. Among the eight discovered isoforms of the *h*-NTPDases, four isoforms, *h*-NTPDase1, -2, -3, and -8, are involved in various physiological and pathological functions, for instance thrombosis, diabetes, inflammation, and cancer. The compound *N*-(4-bromophenyl)-4-chloro-3-(morpholine-4-carbonyl) benzenesulfonamide (**3i**) was found to be the most potent inhibitor of *h*-NTPDase1 with an IC_{50} value of 2.88 ± 0.13 μM. Similarly, the compounds *N*-(4-methoxyphenyl)-3-(morpholinosulfonyl)benzamide (**3f**), 5-(*N*-benzylsulfamoyl)-2-chloro-*N*-(4-methoxyphenyl)benzamide (**3j**) and 2-chloro-*N*-cyclopropyl-5-(*N*-cyclopropylsulfamoyl)benzamide (**4d**) reduced the activity of the *h*-NTPDases2 with IC_{50} in sub-micromolar concentrations. Against the *h*-NTPDase3, **3i** was the potent compound with an IC_{50} concentration of 0.72 ± 0.11 μM. The *h*-NTPDase8 was selectively blocked by the most potent inhibitor 2-chloro-5-(*N*-cyclopropylsulfamoyl)benzoic acid (**2d**) with (IC_{50} = 0.28 ± 0.07 μM). Moreover, the molecular docking studies of the potent inhibitors showed significant interactions with the amino acids of the respective *h*-NTPDase homology model proteins.

Received 9th June 2023
Accepted 4th July 2023

DOI: 10.1039/d3ra03874b

rsc.li/rsc-advances

Introduction

The ectonucleotidases are comprised of four families which include nucleoside triphosphate diphosphohydrolases (*h*-NTPDases), ecto-nucleotide pyrophosphatases/phosphodiesterases (NPPs), ecto-5′-nucleotidase and alkaline phosphatases (ALPs)[1–6] The *h*-NTPDases belong to a diverse group of eight isozymes ranging from *h*-NTPDase1 to *h*-NTPDase8. Each isozyme has a specific capability to catalyse nucleotides. The *h*-NTPDase1, *h*-NTPDase3, and *h*-NTPDase8 have the ability of hydrolysing nucleoside triphosphates as well as nucleoside diphosphates with nearly similar preferences whereas, *h*-NTPDase2 preferentially catalyses the nucleoside triphosphate as substrate.[7] The expression of the *h*-NTPDase isoforms was identified in almost every human body tissue *i.e.* *h*-NTPDase1 is expressed in the subsets of the activated T-cells, monocytes, blood vascular endothelium, and dendritic cells.[4] *h*-NTPDase3 was found in the digestive system (epithelial cells), kidneys, reproductive system, respiratory tract, and islets of Langerhans, whereas, *h*-NTPDase8 was located in the kidney, liver, and intestine.[8–11] Various physiological and pathological functions are associated with the *h*-NTPDases such as regulation of vascular fluidity, cardiac protection, inflammation of vascular vessels, maintenance of thrombosis, and relaxation of vascular vessels. Some unwanted effects due to the irregularity of the *h*-NTPDases include thrombosis, inflammation, diabetes, and cancer.[8,12,13]

Sulfonamides are the most effective chemotherapeutic agents used as anti-hypertensive, anti-bacterial, antiprotozoal, anti-cancer, anti-inflammatory, and anti-diuretic agents.[14] They are mostly considered bacteriostatic and exhibit exceptional anti-bacterial activity against both Gram-positive and Gram-negative bacteria.[15,16] Hence, sulfonamide moieties are used to treat septicaemia, bacillary dysentery, tonsillitis, and urinary

[a]*Department of Chemistry, Quaid-i-Azam University, Islamabad 45320, Pakistan. E-mail: ahassan@qau.edu.pk*

[b]*Centre for Advanced Drug Research, COMSATS University Islamabad, Abbottabad Campus, Abbottabad, Pakistan. E-mail: drjamshed@cuiatd.edu.pk*

[c]*Centre de recherche du CHU de Québec-Université Laval, Québec City, QC, Canada*

[d]*Département de Microbiologie-Infectiologie et d'Immunologie, Faculté de Médecine, Université Laval, Québec City, QC, Canada*

† Electronic supplementary information (ESI) available. See DOI: https://doi.org/10.1039/d3ra03874b

‡ Both authors have equal contribution.

tract infections.[17] They can also lower the blood glucose level and are employed as anti-diabetic agents.

Sulfamoyl-carboxamide is a continually growing class of derivatives possessing valuable and diverse biological activities. Some recent biological activities are reviewed to demonstrate their significance (Fig. 1). NLRP3 is an emerging target for inflammatory diseases such as neuroinflammation, immune inflammation, and metabolic inflammation. NLRP3 is a nucleotide oligomerization domain (NOD)-like receptor protein 3 which is activated by pathogens and damages the cell signal pathway by making NLRP3 inflammasome, a multimeric protein complex.[18] Small molecule sulfonylurea urea such as glyburide (glibenclamide) have been identified as inhibitors for NLRP3 inflammasome.[19] Further modification of the glyburide led to sulfamoyl-benzamide derivatives JC-171 with higher selectivity, increase solubility, and importantly, without affecting the glucose level (Fig. 1).[20] Mincione *et al.* have reported sulfamoyl-benzamides as topically acting carbonic anhydrase inhibitors. These were tested against three isozymes of carbonic anhydrases and showed affinity close to clinical drugs both *in vitro* and *in vivo* as evidenced by compound **I** (Fig. 1).[21] A series of sulfamoyl-4-oxoquinoline-3-carboxamides were screened for defective ΔF508-cystic fibrosis transmembrane conductance regulator (CFTR) chloride channel. Several of the compounds showed correction for CFTR in submicromolar concentration, for instance compound **II** was more effective in comparison.[22] A prominent example is the sulfonylurea-carboxamide based herbicide nicosulfuron, which works at low doses and high selectivity for corn.[23] Zhao *et al.* have reported a series of indole sulfonamide-carboxamide as an excellent inhibitor for wild-type HIV reverse transcriptase through a systematic SAR. The optimization led to compound **III** which was found to have pyrrolidine sulfonamide at position 3 and bromo at position 5 of the indole structure.[24] The 5-chlorosalicylamide scaffold holds biologically interesting properties and the core structure exists in glyburide and JC-171 (*vide supra*), however, Galal *et al.* have found their anti-cancer properties. The sulfamoyl-salicylamide derivatives were tested against five types of human cell lines, while compound **IV** was found to be the best against the breast cancer (MCF-7 and MDA-MB-231) cells (Fig. 1). Furthermore, the tubulin polymerization experiments and flow cytometric assays revealed that compound **IV** resulted in cell cycle arrest by preventing tubulin polymerization.[25]

Considering our interest in finding new inhibitors for *h*-NTPDases,[26,27] and owing to the diverse biological profile of sulfamoyl-carboxamide, synthesis of planned derivatives of sulfamoyl-benzamides was carried out to identify their potential against the activity of the *h*-NTPDase-1, -2, -3, and -8 to develop more effective inhibitors of *h*-NTPDases for the potential treatment of the pathological conditions associated with the unwanted function of the *h*-NTPDases.

Results and discussion

Chemistry

The synthesis of the sulfamoyl-benzamide derivatives is outlined in Scheme 1. We synthesize the 2-substituted benzene sulfonamides-carboxamides through a linear approach, starting from chlorosulfonation of benzoic acids, followed by the sulfonamide and finally the carboxamide synthesis. The chlorosulfonation of the electron-deficient benzoic acid has required slight excess of chlorosulfonic acid and elevated temperature.[28] The corresponding sulfonyl chloride was treated with different amines including cyclopropylamine, morpholine and *p*-bromoaniline for the synthesis of sulfamoylbenzoic acids (**2a–2e**).

The sulfamoyl benzoic acids were subjected to standard carbodiimide coupling conditions using EDC catalytic DMAP in DCM and DMF as co-solvents.[29] The amide coupling generally worked well for anilines and primary and secondary aliphatic amines (Scheme 1). The cyclopropyl sulfonamide **2a** was treated with *p*-chloroaniline and *p*-anisidine for the synthesis of the sulfamoyl-benzamides **3a** and **3b** in 68% and 72% isolated yields, respectively. There was little effect of the electronic nature of the aniline on the amide formation. Similar yields

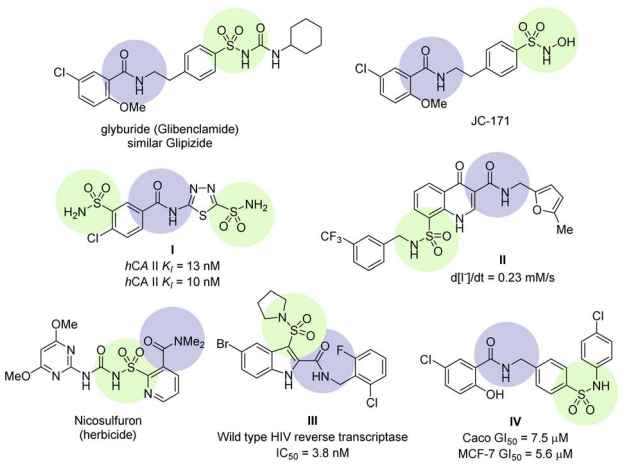

Fig. 1 Selected examples of sulfamoyl-carboxamide containing biologically active compounds.

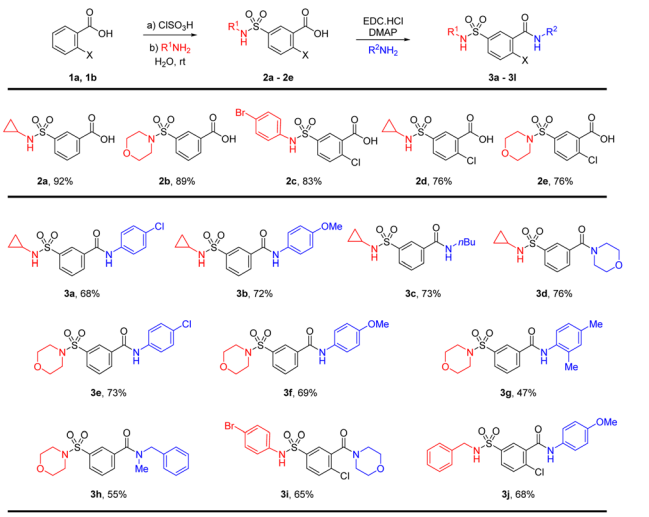

Scheme 1 Linear synthesis of sulfamoyl-benzamide derivatives.

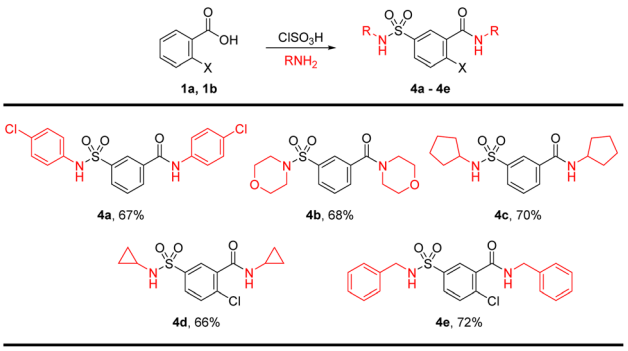

Scheme 2 Direct synthesis of sulfamoyl-benzamide derivatives.

were found for aliphatic amines such as *n*-butylamine and morpholine resulting in product **3c** and **3d**. The morpholino-sulfonamide **2b** was also reacted with *p*-chloroaniline and *p*-anisidine for the synthesis of the benzamides **3e** and **3f** in 73% and 69% yields, respectively. In addition, 2,4-xylidine was able to furnish product **3g** in 47% yield. Further reaction with *N*-methylbenzylamine resulted in the corresponding amide **3h** in 55% yields. The morpholine substituted products **3e–3h** have high polarity and if the *p*H is not properly maintained, the isolation of the product from the aqueous phase may pose a challenge. The *p*-bromoaniline and benzylamine substituted sulfonamides **2c** and **2d** were also converted to amides **3i** and **3j** in good yields (Scheme 1).

To introduce further diversity, a one-pot bis-sulfonamide-carboxamide synthesis resulted in parallel substitutions on either side of the aryl core. To this end, the chlorosulfonation product was telescoped and treated with excess amines for the synthesis of sulfonamide and carboxamide simultaneously for product **4a–4e** in good yields. The bis-amidation was carried out with *p*-chloroaniline, morpholine, pyrrolidine, cyclopropyl-amine, and benzylamine (Scheme 2).

Biological study

Enzyme inhibition assay. The synthesized sulfamoyl derivatives were tested for their enzyme inhibitory potential against the four isoforms of the *h*-NTPDases by using the reported method with minor modifications.[30] The obtained results are presented in Table 1.

Structure–activity relationship. In order to clearly understand the structure–activity relationship (SAR) of the various synthesized benzene sulfonamide-carboxamide derivatives influencing the activity of the *h*-NTPDases isoforms *i.e.*, *h*-NTPDases1, *h*-NTPDases2, *h*-NTPDases3, and *h*-NTPDases8, the derivatives may be divided into three groups depending upon the difference in the structures. Group A: sulfamoylbenzoic acids (**2a–2e**); Group B: sulfamoyl-benzamides (**3a–3j**) and Group C: bis-sulfonamide-carboxamide (**4a–4e**).

Sulfamoylbenzoic acids 2a–2e (Group A). The sulfamoyl group substituted derivatives **2a–2e** tabulated the complex potential to inhibit the activity of either of the *h*-NTPDases isoforms depending upon the nature of the substituted groups. The study of the SAR of the derivatives **2a** and **2b** revealed that *N*-cyclopropyl ring substitution with the sulfonyl group (**2a**) was more favourable for the inhibition of the *h*-NTPDases3 activity (IC_{50} = 1.32 ± 0.06 μM) as compared to the morpholine ring substituted compound **2b** with the sulfonyl group which was devoid of any considerable inhibitory potential against any of the *h*-NTPDases isoenzyme. However, the

Table 1 Presentation of the % inhibition ± S.D or IC_{50} ± SEM (μM) values at 100 μM compound concentration

Codes	*h*-NTPDase1 IC_{50} ± SEM (μM) or % inhibition ± S.D[a]	*h*-NTPDase2 IC_{50} ± SEM (μM) or % inhibition ± S.D[a]	*h*-NTPDase3 IC_{50} ± SEM (μM) or % inhibition ± S.D[a]	*h*-NTPDase8 IC_{50} ± SEM (μM) or % inhibition ± S.D[a]
2a	25 ± 3.2%	10 ± 1.2%	1.32 ± 0.06	24 ± 2.5%
2b	15 ± 2.3%	8 ± 0.7%	35 ± 1.5%	9 ± 3.3%
2c	3 ± 1.2%	22 ± 1.2%	37 ± 2.1%	25 ± 2.4%
2d	3 ± 1.2%	19 ± 0.9%	41 ± 1.4%	0.28 ± 0.07
2e	12 ± 3.4%	15 ± 1.4%	46 ± 1.3%	36 ± 2.3%
3a	5 ± 1.1%	36 ± 1.7%	1.33 ± 0.05	1.78 ± 0.08
3b	34 ± 2.3%	46.91 ± 2.31	46.16 ± 2.41	41.48 ± 2.7
3c	42 ± 1.4%	2.88 ± 0.08	1.49 ± 0.51	46 ± 2.1%
3d	28 ± 2.2%	44 ± 2.3%	41 ± 1.3%	35 ± 2.4%
3e	17.49 ± 1.23	15 ± 1.2%	9 ± 3.2%	24 ± 3.1%
3f	>100	0.27 ± 0.08	6.71 ± 0.04	29 ± 4.5%
3g	26 ± 3.1%	31 ± 3.2%	3.21 ± 0.09	39 ± 3.2%
3h	16 ± 2.3%	32 ± 1.5%	2.54 ± 0.05	38 ± 1.5%
3i	2.88 ± 0.13	43 ± 1.4%	0.72 ± 0.11	32 ± 3.5%
3j	37 ± 1.3%	0.29 ± 0.07	3.16 ± 0.12	36 ± 1.7%
4a	9 ± 2.3%	35 ± 4.6%	22 ± 2.1%	9 ± 2.1%
4b	19 ± 2.2%	25 ± 3.7%	37 ± 3.4%	31.79 ± 2.51
4c	17 ± 4.1%	46.91 ± 2.07	9 ± 1.2%	35 ± 1.2%
4d	36 ± 2.4%	0.13 ± 0.01	0.20 ± 0.07	2.46 ± 0.09
4e	42 ± 1.3%	2.24 ± 0.03	12 ± 2.4%	3 ± 1.2%
Suramin	16.1 ± 1.08	24.1 ± 0.15	4.30 ± 0.84	101.1 ± 2.34

[a] The results are presented as an average of the assays conducted in triplicate. IC_{50} values are determined for the compounds exhibiting over 50% inhibition of enzyme activity; SEM = standard error mean; SD = standard deviation.

selectivity of compound **2a** was moved to *h*-NTPDases8 in case of the presence of chlorine atom at position 2 of the benzene ring in compound **2d**. On the other hand, a comparison of the activity of the **2b** and chlorine substituted **2e** does not enhance the activity of the compound *i.e.*, lower than 50%, suggesting that the attachment with the sulfonyl group is of much importance.

Sulfamoyl-benzamides 3a–3j (Group B). The SAR study of the sulfamoyl-benzamide derivatives differs concerning attachments with the amide group and continuously the cyclopropyl sulfonamide group yielded reliable results. The compound **3a** with chlorophenyl attachment with the amide group significantly reduced the activity of the isoforms *h*-NTPDases3 and *h*-NTPDases8 with IC_{50} values of 1.33 ± 0.05 μM and 1.78 ± 0.08 μM, respectively. However, this activity was reduced to IC_{50} values of 46.16 ± 2.41 μM and 41.48 ± 2.7 μM against the same enzymes for the compound **3b** possessing the methoxyphenyl attachment with the amide group suggesting that the presence of electron withdrawing atom (chlorine) increased the resonance stability of the molecule in **3a** which was much effective for the inhibitory activity as compared to the electron donating methoxy group in compound **3b**. More interestingly, compound **3c** regained the inhibitory potential against the *h*-NTPDases2, *h*-NTPDases3, and *h*-NTPDases8 to the considerable IC_{50} values of 2.88 ± 0.08 μM, 1.49 ± 0.51 μM, and 5.34 ± 0.73 μM, respectively. The increase in the inhibitory potential may be attributed to the presence of the *n*-butyl linkage which enhanced the binding of the **3c** in the hydrophobic region of the enzyme's active site. On the contrary, the presence of the heterocyclic morpholine ring abolished the activity against all four isoforms of *h*-NTPDases.

The observation of the SAR of the compounds **3e–3h** with morpholine ring attached to the sulfonyl group and variation with respect to the amide linkage, the compound **3e** was found although least but selective inhibitor of the *h*-NTPDase1 which blocked the activity presenting the IC_{50} = 17.49 ± 1.23 μM, whereas the molecule **3f** more specifically inhibited the activity of the isoform with IC_{50} values equals 0.27 ± 0.08 μM. The two compounds **3g** and **3h** selectively reduced the activity of the *h*-NTPDase3 to almost equal extent *i.e.*, 3.21 ± 0.09 μM and 2.54 ± 0.05 μM. The effect of the compounds **3g** and **3h** may be attributed to the presence of the methyl and methylene groups which contributed to the sigma bond hyperconjugation bonding effect to interact with the amino acids of the *h*-NTPDase3 catalytic site. The presence of the two halogen atoms chlorine and bromine in the structure **3i** (IC_{50} = 2.88 ± 0.13 μM) led the compounds towards the most potent and single active molecule against the isoform *h*-NTPDase1. Comparison of the SAR of the compounds **3e** and **3i** against the *h*-NTPDase1 revealed that the presence of the two halogen atoms on the chemically almost similar structures enhanced the activity of compound **3i** to a greater extent. The compound **3j** preferentially blocked the activity of the *h*-NTPDase2 demonstrating the IC_{50} concentration of 0.29 ± 0.07 μM in accordance with the **3f** which reduced the *h*-NTPDase2 activity to the same level. The *h*-NTPDase2 inhibitory effect of the **3j** might be attributed to the presence of the methoxy group and the additional potency of the **3j** to inhibit the *h*-NTPDase3 could be due to the presence of the methylene group like the structures **3g** and **3h**.

Bis-sulfonamide-carboxamide 4a–4e (Group C). The attachment of the chlorophenyl scaffolds on both sides of the molecules as in compound **4a**, abolished the activity of the **4a** against any of the *h*-NTPDases isoforms which can be argued that the presence of the chlorophenyl ring on the single side of the molecule was effective. The almost reduced potency was noted in compound **4b** possessing morpholine ring and compound **4c** with cyclopentyl ring on both sides of the compound. However, a completely opposite result was obtained in case of cyclopropyl on both sides of the molecule **4d**, which retrieved the activity for the *h*-NTPDases2, *h*-NTPDases3 and *h*-NTPDases8 to an IC_{50} value of 0.13 ± 0.01 μM, 0.20 ± 0.07 μM, and 2.46 ± 0.09 μM, tabulating the most potent inhibitor of the *h*-NTPDases2, and *h*-NTPDases3 among the synthesized compounds suggesting that the small cyclic rings are effective for the activity of the compounds.

Molecular docking study

For the purpose to predict the plausible mode of interaction of selected inhibitors of each isoform *i.e.*, *h*-NTPDase1, *h*-NTPDase2, *h*-NTPDase3, and *h*-NTPDase8, the molecular docking study was carried out by using the homology models. Followed by the docking of the compounds with respective proteins, the most reliable pose which showed a significant binding affinity with the amino acid residues was selected to visualize.

Molecular docking studies at *h*-NTPDase1. The molecular docking studies of the most active inhibitor **3i** against the *h*-NTPDase1 revealed the interactions with several amino acid residues Trp450, Asp54, Tyr63, Phe360, Ile182, and Ser361 in accordance with the reported literature.[31] These interactions were comprised of van der Waals forces, hydrogen bonding, π-alkyl, and π–π stacked forces. Apparently, the residues Trp450, Asp54, and Tyr63 were connected with the morpholine ring of inhibitor **3i** through hydrogen bonding. A single π–π stacked interaction was observed between amino acid Phe360 and π-electrons of the phenyl ring of the bromo-phenyl scaffold. Moreover, the bromine atom was connected with the Ile182 and Phe360 *via* alkyl and π-alkyl interactions, respectively as depicted in Fig. 2a.

Molecular docking studies at *h*-NTPDase2. In the case of the molecular docking of the most potent inhibitor of *h*-NTPDase2 shown that molecule **3f** was surrounded by an array of multiple bonds (Fig. 2b). The previously reported amino acids such as: His50, Tyr350, Ser346, Arg245, Arg392, Ala393, and Ala347 were found in interactions with the molecule **3f**.[32] The H-bonding were observed among the His50 – morpholine ring, Asp45 – morpholine ring, Ser52 – morpholine ring, Ser346 – oxygen atom of sulfonyl group, and between the residue Arg392 and oxygen atom of acetamide moiety. The sulfur atom of the sulfonyl group was found in linkage with the residue Tyr350. The phenyl rings of the inhibitor **3f** were surrounded by the residues His50 and Tyr350 through the π–π interaction, and by

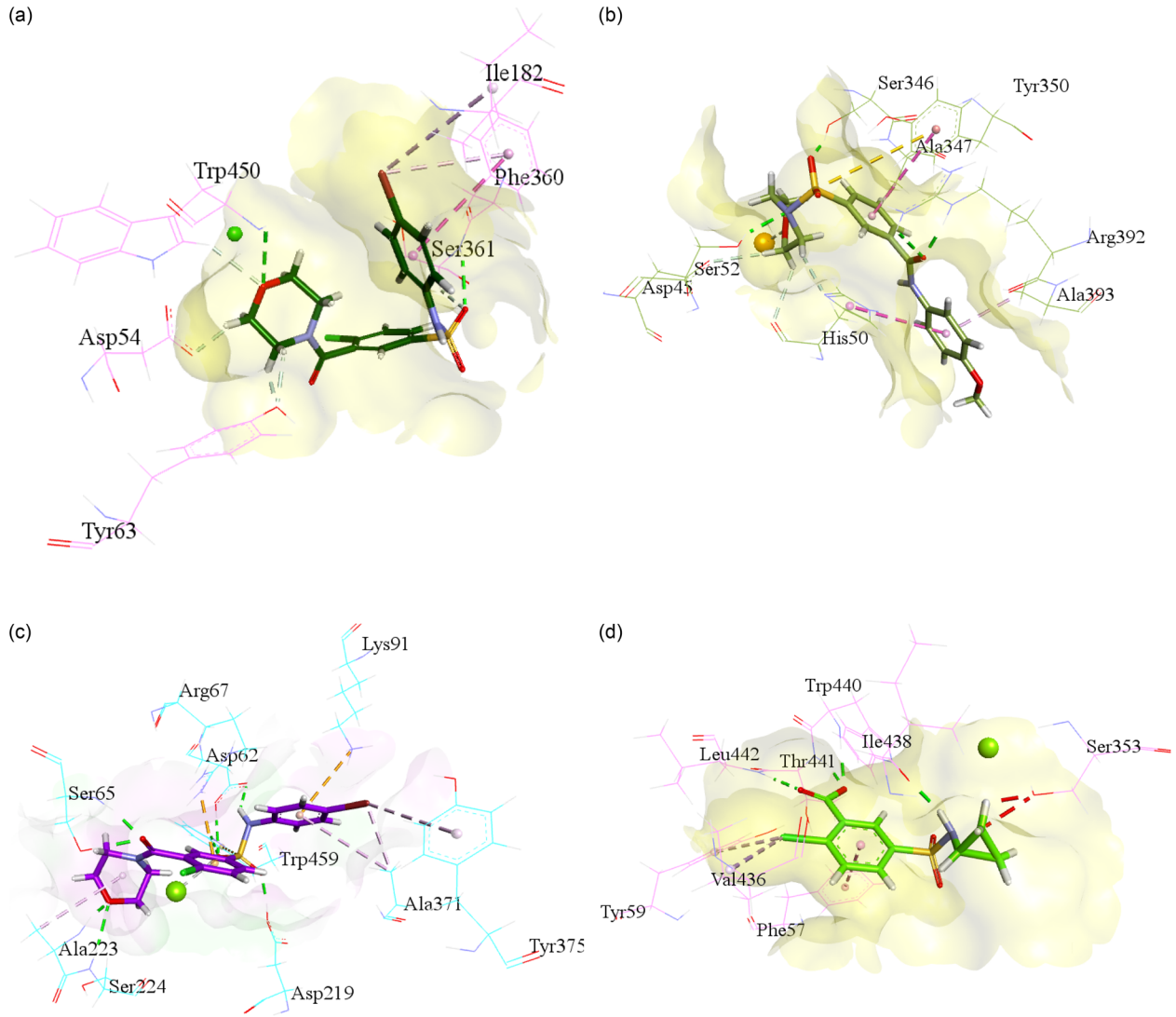

Fig. 2 Illustration of molecular docking of the most potent NTPDases inhibitor against modelled *h*-NTPdase1, *h*-NTPdase2, *h*-NTPdase3, and *h*-NTPdase8. (a) Illustration of the plausible mode of interaction of compounds **3i** within the *h*-NTPDase1 catalytic site. (b) Illustration of the plausible mode of interaction of compounds **3f** within the *h*-NTPDase2 catalytic site. (c) Illustration of the plausible mode of interaction of compounds **3i** within the *h*-NTPDase3 catalytic site. (d) Illustration of the plausible mode of interaction of compounds **3i** within the *h*-NTPDase8 catalytic site.

the residues Ala393 and Ala347 *via* the π-alkyl linkage. Moreover, the oxygen atom of the morpholine ring formed metal chelation with the calcium ion of the protein.

Molecular docking studies at *h*-NTPDase3. The molecular docking study of the active inhibitor **3i** with the isoform *h*-NTPDase3, was performed by using the homology model of protein *h*-NTPDase3. A visualization of the binding pattern of molecule **3i** declared a complex sequence of interactions with the amino acid residues as highlighted in the reported study (Fig. 2c).[29] These interactions include hydrogen bonding, π-cation, π-sulfur, alkyl, and π-alkyl linkages. The hydrogen bonding was found among Ala223, Ser224, and morpholine scaffold; Ser65 and the oxygen atom of the amide group; Asp219, Trp459 and oxygen atoms of the sulfonyl group; Trp459 and the oxygen atom of the sulfonyl group; Asp62 and the oxygen atom of sulfonyl group; Asp62 and hydrogen atom of –NH moiety. Both aromatic rings were connected *via* π electrons to the important amino acids Arg67 and Lys91 through π-cation linkage. Similarly, the sulfur atom of inhibitor **3i** was found to be connected with the π electrons of the phenyl ring of the residue Trp459. Moreover, metal chelation was observed between the magnesium metal ion and the oxygen atom of the sulfamoyl group of compounds **3i**.

Molecular docking studies at *h*-NTPDase8. The docking conformation of the inhibitor **2d** and the place of binding interactions within or around the *h*-NTPDase8 active site is shown in Fig. 2d. The binding site of the protein *h*-NTPDase8 is comprised of the important amino acid residues such as Phe57, Tyr59, Tyr178, Gly179, Gly435, Ile438, Val436, Thr441, and Leu442 comprising.[26,29] The oxygen and hydrogen atoms of the

carboxylic group were involved in the H-bond formation with the residues Trp440, Thr441, and Leu442, moreover, the hydrogen atom attached with the nitrogen atom of the sulfamoyl group was also connected *via* H-bond interaction with the amino acid Ile438. A π–π stacked connection was found between the aromatic ring and the Phe57, a π-alkyl interaction was observed among the chlorine atom of the chlorophenyl ring and the Tyr59, and an alkyl bridge was located between the chlorine atom and the residue Val436. Most importantly, an unfavourable bump was present between the cyclopropyl ring and the residues Ser353 which demonstrate the high binding affinity of the molecule **2d** with the active site residues.

Conclusions

In conclusion, the sulfamoylbenzoic acids (**2a–2e**), sulfamoylbenzamides (**3a–3j**), and bis-sulfonamide-carboxamide (**4a–4e**) were synthesized and tested for their effect on the activity of the *h*-NTPDase1, *h*-NTPDase2, *h*-NTPDase3, and *h*-NTPDase8. As a result, many potent and selective inhibitors of each isozyme were found which blocked the activity from micromolar to submicromolar concentrations. The compound **3i** (IC_{50} = 2.88 ± 0.13) was obtained as most potent inhibitor of *h*-NTPDases1; compounds **3f** (IC_{50} = 0.27 ± 0.08 μM), **3j** (IC_{50} = 0.29 ± 0.07 μM) and **4d** (IC_{50} = 0.13 ± 0.01 μM) preferably reduced the function of the *h*-NTPDase2. The potent inhibitor of *h*-NTPDase1 (**3i**) was also very active against the activity of the *h*-NTPDase3 with IC_{50} concentrations equal to 0.72 ± 0.11 μM and the compound **2d** selectively blocked the activity of the *h*-NTPDase8 presenting the IC_{50} value of 0.28 ± 0.07 μM. Moreover, the molecular docking interactions of the most potent compounds with the amino acid residues of the *h*-NTPDases proteins justified the *in vitro* results. In short, the molecules screened as potent and selective inhibitors of the *h*-NTPDases isozymes may be further evaluated as drug candidates against the diseases associated with the aberrant activity of these enzymes.

Experimental

Synthesis of the compounds

The detailed procedure for the synthesis of the sulfamoylbenzamides and their analytical data is given in the ESI† file.

Biological section

Enzyme inhibition assay *h*-NTPDases. The sulfamoyl derivatives were tested for their enzyme inhibitory potential against the four isoforms of the *h*-NTPDases by using the previously reported method with minor modifications.[30] The malachite green assay was performed in an assay buffer which was composed of the components such as 5 mM of calcium chloride, and 50 mM of tris-hydrochloric acid maintained to a *p*H of 7.4 at room temperature. The compounds were examined in triplicate at the concentration of 100 μM for each well. The incubation time of 10 min was given to the assay plate containing the assay buffer, 100 μM of the compound, 12 ng of *h*-NTPDase1, or 37 ng of *h*-NTPDase2, or 43 ng of *h*-NTPDase3, and 63 ng of *h*-NTPDase8. After taking the reading with the assistance of microplate reader Omega FLUOstar microplate reader (BMG Labtech, Germany) at 630 nm, the substrate (100 μM) was added to initiate the reaction and incubated for 15 min at a temperature of 37 °C. After 15 min incubation, malachite green reagent (15 μL) was added to each well and reading was noted up to 6 min. The % enzyme inhibition results were calculated and the inhibitors which showed above 50% reduction of the respective enzyme were subjected to the serial ascending concentrations and half of the maximal compound concentration (IC_{50}) was determined by using PRISM 5.0 (GraphPad, San Diego, California, USA).

Molecular docking study. Due to the unavailability of the crystallographic structures of the *h*-NTPDases, the already developed homology models were used for molecular docking study.[33] The structures of the compounds were drawn by using ChemDraw software and energy was minimized with the help of MOE (Molecular Operating Environment). The compounds were saved in Mol2 formats for docking studies in the active pocket of the enzyme.[34] The preparation of proteins, selection of the active pocket, and other parameters were selected by using the software LeadIT (BioSolveIT GmbH, Germany) and molecular docking study was carried out.[35] The 50 poses for each ligand were visualized and the ligand showing the highest binding affinity and low interaction energy were selected with the help of Discovery Studio Visualizer DS.[36]

Conflicts of interest

We have no conflicts of interest to disclose.

Acknowledgements

AH is grateful to the Higher Education Commission (HEC) Pakistan for NRPU research grant 20-3885/R&D/HEC/14. JI acknowledges the financial support provided by the HEC *via* NRPU project No. 20-15846/NRPU/R&D/HEC/2021.

Notes and references

1 I. Grković, D. Drakulić, J. Martinović and N. Mitrović, *Curr. Neuropharmacol.*, 2019, **17**, 84–98.
2 S.-Y. Lee and C. E. Müller, *MedChemComm*, 2017, **8**, 823–840.
3 S.-Y. Lee, S. Sarkar, S. Bhattarai, V. Namasivayam, S. De Jonghe, H. Stephan, P. Herdewijn, A. El-Tayeb and C. E. Müller, *Front. Pharmacol.*, 2017, **8**, 54.
4 D. D. Nabinger, S. Altenhofen and C. D. Bonan, *Prog. Neuro-Psychopharmacol. Biol. Psychiatry*, 2020, **98**, 109770.
5 M. Tozzi and I. Novak, *Front. Pharmacol.*, 2017, **8**, 878.
6 H. Ahmad, S. Ullah, F. Rahman, A. Saeed, J. Pelletier, J. Sévigny, A. Hassan and J. Iqbal, *Eur. J. Med. Chem.*, 2020, **208**, 112759.
7 K. Hayat, S. Afzal, A. Saeed, A. Murtaza, S. Ur Rahman, K. M. Khan, A. Saeed, S. Zaib, J. Lecka, J. Sévigny, J. Iqbal and A. Hassan, *Bioorg. Chem.*, 2019, **87**, 218–226.

8 A. J. Marcus, M. J. Broekman, J. H. F. Drosopoulos, K. E. Olson, N. Islam, D. J. Pinsky and R. Levi, *Semin. Thromb. Hemostasis*, 2005, **31**, 234–246.
9 G. Kauffenstein, C. R. Fürstenau, P. D'Orléans-Juste and J. Sévigny, *Br. J. Pharmacol.*, 2010, **159**, 576–585.
10 S. C. Robson, J. Sévigny and H. Zimmermann, *Purinergic Signalling*, 2006, **2**, 409–430.
11 F. Kukulski, S. A. Lévesque and J. Sévigny, in *Advances in Pharmacology*, ed. K. A. Jacobson and J. Linden, Academic Press, 2011, vol. 61, pp. 263–299.
12 C. E. Müller, J. Iqbal, Y. Baqi, H. Zimmermann, A. Röllich and H. Stephan, *Bioorg. Med. Chem. Lett.*, 2006, **16**, 5943–5947.
13 S. Afzal, M. al-Rashida, A. Hameed, J. Pelletier, J. Sévigny and J. Iqbal, *Front. Pharmacol.*, 2020, **11**, 585876.
14 Y. Lavanya, *Int. J. Pharm. Sci. Invent.*, 2017, **6**, 1–3.
15 S. Seino, *Diabetologia*, 2012, **55**, 2096–2108.
16 Y. Ö. Genç and Y. Reşit Bekdemir, *Ann. Clin. Microbiol. Antimicrob.*, 2008, **7**, 1–6.
17 M. H. Mengelers and Janssen, *J. Vet. Pharmacol. Ther.*, 1997, **20**, 276–283.
18 X. Zhang, A. Xu, J. Lv, Q. Zhang, Y. Ran, C. Wei and J. Wu, *Eur. J. Med. Chem.*, 2020, **185**, 111822.
19 M. Lamkanfi, J. L. Mueller, A. C. Vitari, S. Misaghi, A. Fedorova, K. Deshayes, W. P. Lee, H. M. Hoffman and V. M. Dixit, *J. Cell Biol.*, 2009, **187**, 61–70.
20 C. Guo, J. W. Fulp, Y. Jiang, X. Li, J. E. Chojnacki, J. Wu, X.-Y. Wang and S. Zhang, *ACS Chem. Neurosci.*, 2017, **8**, 2194–2201.
21 F. Mincione, M. Starnotti, L. Menabuoni, A. Scozzafava, A. Casini and C. T. Supuran, *Bioorg. Med. Chem. Lett.*, 2001, **11**, 1787–1791.
22 Y. F. Suen, L. Robins, B. Yang, A. S. Verkman, M. H. Nantz and M. J. Kurth, *Bioorg. Med. Chem. Lett.*, 2006, **16**, 537–540.
23 K. R. Darren, W. M. David and R. S. Jonathan, *Weed Technol.*, 1994, **8**, 630–634.
24 Z. Zhao, S. E. Wolkenberg, M. Lu, V. Munshi, G. Moyer, M. Feng, A. V. Carella, L. T. Ecto, L. J. Gabryelski, M.-T. Lai, S. G. Prasad, Y. Yan, G. B. McGaughey, M. D. Miller, C. W. Lindsley, G. D. Hartman, J. P. Vacca and T. M. Williams, *Bioorg. Med. Chem. Lett.*, 2008, **18**, 554–559.
25 A. M. F. Galal, M. M. Soltan, E. R. Ahmed and A. G. Hanna, *MedChemComm*, 2018, **9**, 1511–1528.
26 G. Zaman, S. Ullah, M. Uzair, S. Batool, H. Ahmad, F. Ullah, J. Pelletier, J. Sévigny, J. Iqbal and A. Hassan, *ChemMedChem*, 2023, e202300165.
27 Z. Begum, S. Ullah, M. Akram, M. Uzair, F. Ullah, Ahsanullah, J. Pelletier, J. Sévigny, J. Iqbal and A. Hassan, *Bioorg. Chem.*, 2022, **129**, 106196.
28 J. P. Bassin, R. J. Cremlyn and F. J. Swinbourne, *Phosphorus, Sulfur Silicon Relat. Elem.*, 1991, **56**, 245–275.
29 A. Murtaza, S. Afzal, G. Zaman, A. Saeed, J. Pelletier, J. Sévigny, J. Iqbal and A. Hassan, *Bioorg. Chem.*, 2021, **115**, 105240.
30 S. A. Lévesque, É. G. Lavoie, J. Lecka, F. Bigonnesse and J. Sévigny, *Br. J. Pharmacol.*, 2007, **152**, 141–150.
31 M. Zebisch, M. Krauss, P. Schäfer and N. Sträter, *J. Mol. Biol.*, 2012, **415**, 288–306.
32 M. Zebisch and N. Sträter, *Proc. Natl. Acad. Sci.*, 2008, **105**, 6882–6887.
33 J. Iqbal and S. J. A. Shah, *Sci. Rep.*, 2018, **8**, 2581.
34 *MOE (Molecular Operating Environment) Version 2019.0201*, Chemical Computing Group (CCG), 2019.
35 *LeadIT version 2.3.2*, BioSolveIT GmbH, Sankt Augustin, Germany, 2017.
36 Dassault Systemes BIOVIA, *Discovery Studio Modeling Environment, Release 2017*, Dassault Systemes, San Diego, 2016.